Since January 2020 Elsevier has created a COVID-19 resource centre with free information in English and Mandarin on the novel coronavirus COVID-19. The COVID-19 resource centre is hosted on Elsevier Connect, the company's public news and information website.

Neuroscience Informatics 2 (2022) 100069

Contents lists available at ScienceDirect

Neuroscience Informatics

www.elsevier.com/locate/neuri

Artificial Intelligence in Brain Informatics

A novel approach for detection of COVID-19 and Pneumonia using only binary classification from chest CT-scans

Sanskar Hasija, Peddaputha Akash, Maganti Bhargav Hemanth, Ankit Kumar, Sanjeev Sharma *

Indian Institute of Information Technology, Pune, India

ARTICLE INFO

Article history:
Received 15 March 2022
Accepted 22 March 2022

Keywords:
COVID-19
Chest CT scan
CNN
Two binary classifications
Multiclass classification
Classification metrics

ABSTRACT

The novel Coronavirus, Severe Acute Respiratory Syndrome Coronavirus 2 (SARS-CoV-2) spread all over the world, causing a dramatic shift in circumstances that resulted in a massive pandemic, affecting the world's well-being and stability. It is an RNA virus that can infect both humans as well as animals. Diagnosis of the virus as soon as possible could contain and avoid a serious COVID-19 outbreak. Current pharmaceutical techniques and diagnostic methods tests such as Reverse Transcription-Polymerase Chain Reaction (RT-PCR) and Serology tests are time-consuming, expensive, and require a well-equipped laboratory for analysis, making them restrictive and inaccessible to everyone. Deep Learning has grown in popularity in recent years, and it now plays a crucial role in Image Classification, which also involves Medical Imaging. Using chest CT scans, this study explores the problem statement automation of differentiating COVID-19 contaminated individuals from healthy individuals. Convolutional Neural Networks (CNNs) can be trained to detect patterns in computed tomography scans (CT scans). Hence, different CNN models were used in the current study to identify variations in chest CT scans, with accuracies ranging from 91% to 98%. The Multiclass Classification method is used to build these architectures. This study also proposes a new approach for classifying CT images that use two binary classifications combined to work together, achieving 98.38% accuracy. All of these architectures' performances are compared using different classification metrics.

1. Introduction

There are lots of viruses in the corona family that may be found in animals such as camels, bats, and pigs. Out of these numerous coronaviruses seven are threatening to humans. The SARS-Cov-2 was initially transmitted from bats which caused severe acute respiratory disease and emerged as the largest pandemic in the world [9]. As a result of this pandemic, researchers at several R&D laboratories are actively engaged in timely detection, proper analysis of the virus, and vaccination for treatment. After entering the respiratory tract of a human, novel coronavirus causes respiratory deterioration and may even lead to pneumonia. COVID infected lungs were found to produce "Ground-Glass Opacity (GGO)" patches and to be filled with mucus fluid [32]. Various symptoms make it more difficult to diagnose the disease in the first place and the limited availability of test kits and the disposable nature of these kits make it harder to perform PCR tests. Another drawback is the rise in the number of True Negative or False Negative values results, which together shows that an alternative diagnostic technique should be used. CT scans are found to be providing better results in the current scenario and they are 5 times cheaper than PCR tests [21].

Deep Learning (DL) may be a subset of Machine Learning (ML) which successively may be a subset of Artificial Intelligence (AI). Deep Learning is a type of ML inspired by the structure of the Human Brain which in Deep Learning is called an Artificial Neural Network. It learns features and tasks directly from data (Data can be of any form viz., Image, text, or sound). It is an end-to-end learning as the task is to learn directly from data. Traditional Neural Networks contain 2 or 3 hidden layers whereas the latest networks are as deep as 150 layers.

Chest X-Ray [14,20,6] and CT scans provide promising results but they are usually interpreted by expert radiologists. As several patients visit radiologists every day and the diagnosis process takes a great deal of time, discrepancies can rise dramatically which de-

* Corresponding author.
E-mail addresses: sanskarhasija19@cse.iiitp.ac.in (S. Hasija), akashpeddaputha19@cse.iiitp.ac.in (P. Akash), bhargavmaganti19@cse.iiitp.ac.in (M. Bhargav Hemanth), ankitkumar19@cse.iiitp.ac.in (A. Kumar), sanjeevsharma@iiitp.ac.in (S. Sharma).

https://doi.org/10.1016/j.neuri.2022.100069

picts the need for Computer-Aided Diagnostic (CAD) to decrease false negatives and also save time and money. Moreover, automated DL-based CAD tools are considered to work exceptionally well in pulmonary disease detection [17].

Convolutional Neural Network (CNN) is a Deep Learning Neural Network that has turned out to be performing remarkably in the analysis of documents, classification of various images, detection of the pose, and action. It also performs impressively in the area of medical imaging [28,25]. So, CNN models can be used to make better predictions on images [5,3].

The dataset used in this study comprises three distinct sets of CT slices: normal, pneumonia, and COVID-19. Most of the previous research proposed multiclass classifiers, but the current study proposed a new approach that focuses on building a model that works in two phases. The first phase is to divide the CT slices into two categories: COVID-19 and NON-COVID, with Normal and Pneumonia CT slices falling into the NON-COVID-19 group. If the first phase's output is COVID-19, the process stops there; otherwise, the output goes on to the next phase. The output of the first step would be the input to the second stage, and the possible outcomes are Normal and Pneumonia.

The main objectives of this study are:

- To demonstrate the performance of various models, including AlexNet, ResNet152-V2, MobileNet-V2, and VGG-19, as well as to suggest a new approach to data classification.
- Design a model to differentiate CT scans into three different classes i.e., Normal, Pneumonia, COVID in two phases.
- Augmentation of data for better results on the validation set of data on the above models.
- Computing and analyzing various classification metrics such as sensitivity, positive predictive value, F1 score, specificity, and model accuracy.

The rest of the paper is structured as follows: Section 2 addresses the problem's associated work. Section 3 goes through the methodology, which includes database collection, preprocessing, deep learning model design, and parameter setup. Section 4 delves into the experimental findings and interpretation. At last, we will be concluding the work in Section 5.

2. Related work

The key advantage of AI-based platforms is that they speed up the diagnosis and treatment of COVID-19 disease [15]. CNN has a wide range of applications, including object detection and image classification, as well as medical imaging. Alexnet, ZFNet, and VGGNet are a few well-known CNN models for image classification that perform well in real-world situations [35,16,26]. Predictions obtained from trained models based on laboratory results might be used to detect COVID-19 infection and assist health professionals in properly allocating resources [4]. Gunraj proposed two models (COVID-Net CT & COVID-Net CT-2) [11,10] using COVIDx CT-2A data set and achieved 97.9% and 98.1% accuracy respectively and set benchmark results while training a model with such a large data set. Anomalies or ROI in the CT scan were visualized using Gradient-weighted Class Activation Mapping (Grad-CAM) [23]. The test results reveal that the predictive models suggested by [4] definitively diagnose patients with COVID-19 disease with an accuracy of 86.66%, F1-score of 91.89%, the precision of 86.75%, recall of 99.42%, and AUC of 62.50%. Toğaçar et al. [29], which is a combination of MobileNetV2 and SqueezeNet, reached a 99.27% accuracy.

The Social Mimic optimization method was used to process the feature sets generated by the models. Following that, Support Vector Machines were used to blend and classify effective features (SVM). The experimental results demonstrated that the model suggested by [27] can reliably distinguish COVID-19 patients from others, with an AUC of 0.99 and recall (sensitivity) of 0.93. Furthermore, with an AUC of 0.95 and a recall (sensitivity) of 0.96, this model was capable of distinguishing COVID-19 infected patients from bacteria pneumonia-infected patients. Yadav and Jadhav [34] used pneumonia data, Support Vector Machine (SVM) as a classification method, and InceptionV3, VGG-16 models as a deep learning approach to execute a classification algorithm. Their study's dataset was categorized into 3 classes: normal, bacterial pneumonia, and viral pneumonias. Data Augmentation was also used to enhance the contrast, brightness, and zoom presets of each image in the dataset. The best classification achievement was 96.6%. Haque and Abdelgawad [12] suggested a combination of ResNet, VGG-16, and VGG-19 model for COVID detection, which attained an accuracy of 98.3% after being trained with 1356 images. Panwar et al. [22]s proposed an algorithm that helps models detect COVID faster, and implementing the algorithm on VGG-16 yielded an overall accuracy of 88.10% and COVID prediction accuracy of 97.62%.

3. Materials and methods

3.1. Data collection and modeling

COVIDx CT [11] is a fully accessible benchmark data set comprising 1,94,922 CT slices from 3,745 patients derived from publicly – accessible databases. Our model is trained, tested, and validated using this data set. This data set was made available on 'Kaggle' on September 13, 2020. COVIDx CT is licensed under a CC BY-NC-SA 4.0 license, which is consistent with the licensing of its constituent datasets.

COVIDx CT is available in two versions:

'A' and 'B.' Cases with a confirmed diagnosis make up the 'A' variant. CT slices containing anomalies in NON-COVID-19 pneumonia and COVID-19 cases were detected either a) manually by radiologists or b) manually by non-radiologists. The 'B' variant includes the entire 'A' variant as well as some cases that are believed to be properly diagnosed but cannot be confirmed. This data set provides 1,43,778 images for training the model (which has 82,286 images of covid +ve scans, 25,496 images of pneumonia scans, and 35,996 images of normal scans), 25,658 images for testing (6,018 covid +ve scans, 7,395 images of pneumonia scans, 12,245 images of normal scans) and 25,486 validation data (6,244 images of covid +ve scans, 7,400 images of pneumonia scans, 11,842 images of normal scans).

Fig. 1a and 1b are bar graphs representing image distribution among train, test & validation data set for phase-1 and phase-2 respectively. To create a Deep Learning model, data plays an integral role, and proper data training is essential to accomplish greater accuracy. Our model is trained, tested, and validated using this data set. Since the proposed model consists of two stages, the data is also divided into two parts. The data for the training phase-1 is divided into NON-COVID and COVID categories, with the NON-COVID class comprising both Normal and Pneumonia CT slices. The total number of NON-COVID images used in this study is 61,599 (25,515 Pneumonia CT slices and 36,084 Normal CT slices) with 50,000 images of COVID CT slices chosen at random to preserve data balance. In the second training phase, the data was split into Normal and Pneumonia categories with the same number of images used as above. The image's original dimensions were 512×512, and they include bounding boxes that serve as the Region of Interest (ROI). The images were reduced to the ROI and then resized to a shape of 128×128.

Fig. 2 depicts sample CT-Scan images of all three classes i.e. Normal, COVID-19, Pneumonia respectively. To meet the require-

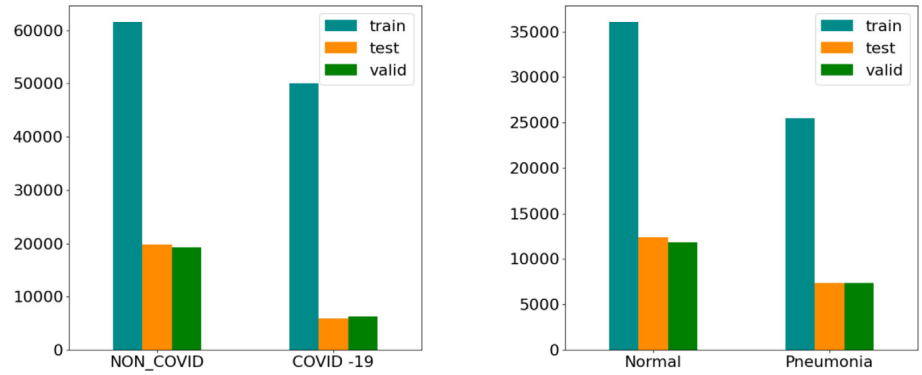

(a) Image distribution of COVID & Non-COVID Data (b) Image distribution of Normal & Pneumonia Data

Fig. 1. Image Distribution for Phase-1 and Phase-2.

(a)Normal class CT-scan (b) Pneumonia class CT-scan (c) COVID-19 class CT-scan

Fig. 2. Example CT-scan images from the training dataset of all 3 classes.

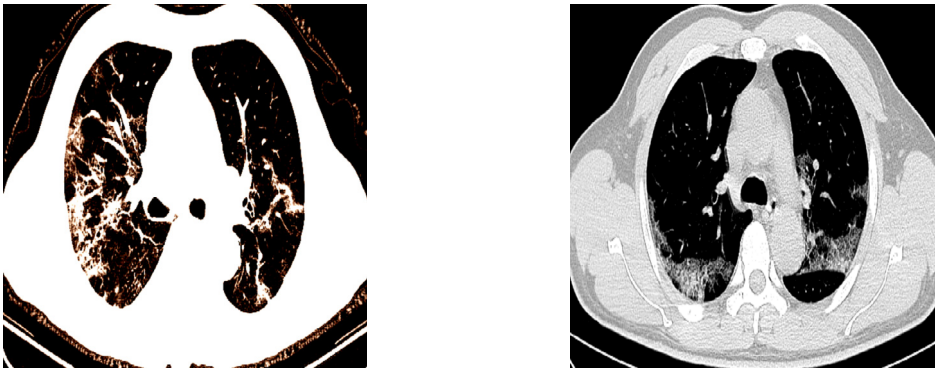

(a) Example Pre-Processed image for Phase-1 training (b) Example Pre-Processed image for Phase-2 training

Fig. 3. Pre-Processed Images for Training Phases.

ments needed by various models, the images were further preprocessed by passing them through the model-specific preprocessing function provided by the Keras library. Fig. 3a and 3b represents pre-processed images for Phase-1 and Phase-2 training, respectively. The data was then augmented with various parameters like rotation range, shear range, height shift range, width shift range, zoom range, and horizontal flip etc.

3.2. CNN architecture

Convolutional Neural Networks are designed efficiently and adaptively by integrating spatial feature hierarchies via backpropagation using numerous key components such as convolution layers, pooling layers, and fully connected layers (FCC). They have become prominent in a variety of computer vision applications and are attracting interest in a multitude of disciplines, including radiology [36]. Therefore, CNNs are used while building both the phases of the proposed model. The phase-1 model and phase-2 model are two sequential CNNs suggested. Phase-1 model is used to classify the data into 2 categories either Covid or NON-COVID. After the phase-1, NON-COVID images can be classified into categories of either normal or pneumonia by phase-2 model (Fig. 4). So, both phase-1 and phase 2 do binary classification of data. Figs. 5 and 6 represent the Phase-1 and Phase-2 versions, respectively.

Phase-1 is made up of five components:

1. Grouping of NON-COVID data
2. Input layers
3. Densenet-201 base model
4. Fully Connected Layers with dropout
5. The Output Layer

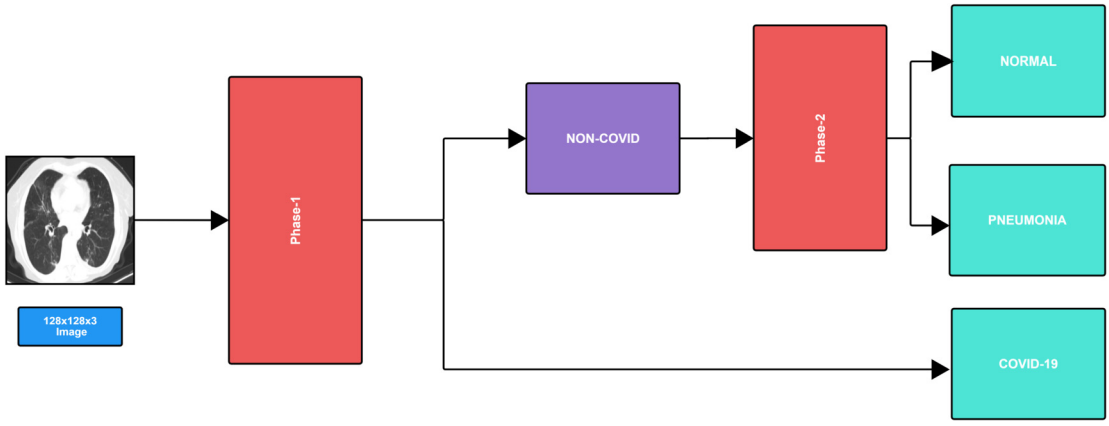

Fig. 4. Flowchart depecting workflow of the Model.

The images from the normal and pneumonia classes were combined and labeled as NON-COVID image sets. The model's input layer received both NON-COVID and COVID-19 images. The input layer was then connected to the DenseNet-201 model which was imported from Keras library using Trans205 fer Learning technique [31]], which was used as the base model and was pre-trained on the ImageNet dataset [8]].

DenseNet-201 was also connected to a Global Average Pooling layer (GAP) [18]. A Global Average Pooling layer was used over Flatten because flatten essentially re-arranges the elements of a multi-dimensional object to make it one-dimensional, while Global average pooling employs a parser window that passes across the object and pools the data by averaging it. GAP acts as a link between CNN layers and FCC layers by flattening the output and passing it as a 1-D array to the next layers. The subsequent layer was a dense layer with 64 characteristics that was accompanied by a dropout layer with a 20% probability. In the Dense Layer, ReLu activation was used because ReLu activation function is much faster which makes a massive improvement in neural network training and prediction time. The dropout layers aid in reducing training data overfitting. The final layer is a sigmoid layer that provides two predicted probabilities of the two classes that add up to one. The final layer determines whether an image is a positive or negative image. The total number of trainable parameters in the phase-1 sequential model was 18,215,937.

Since Phase 2 did not include any image grouping for a specific class, it has four components. Four Components of Phase-2:

1. Input layers
2. Inception V3 base model
3. Fully Connected Layers with dropout
4. The Output Layer

The two-image classes were Normal and Pneumonia. These classes were both given in the input layers. The input layer was also connected to the InceptionV3 model, which served as the base model and was pre-trained on the ImageNet dataset. The InceptionV3 base model was further connected to the Global Average Pooling layer. The following layer was a dense layer with 128 features, which was followed by a dropout layer with a 30% probability. In the Dense Layer, ReLu activation was used. The dropout layers lessen training data from overfitting. The final layer is a sigmoid layer that provides two predicted probabilities of the two classes that add up to one. The final layer predicts whether an image is positive or negative for Pneumonia. The total number of trainable parameters in the phase 2 sequential model was 22,030,753. In contrast to the proposed model, which had two binary classifications, the ResNet152V2, MobileNetV2, AlexNet, and VGG-19 models were designed with multiclass classification, which categorized the output into three categories – Normal, Pneumonia, and COVID-19. The respective model's ImageNet weights were used to train these models. As illustrated in the Fig. 7.

3.3. Implementation (parameter selection)

Since the model was constructed in two phases, hyperparameters were chosen accordingly. For phase-1, the data was divided into two categories: NON-COVID and COVID, with 50,000 images chosen at random from the COVID category to ensure data balance. The data was divided into batches of size 32. The total number of epochs was 70. For the first 40 epochs, the learning rate was set to 0.0001 and then raised by 10 times for the subsequent epochs. We utilized cropping box jitter, rotation, horizontal and vertical shear, horizontal flip, and intensity shift and scaling to augment the data for better results. Except for the data augmentation, all of the hyperparameters remained unchanged for the second phase. The proposed model was designed, trained, and evaluated using the TensorFlow [1] machine learning library on the online cloud workspace FloydHub.

4. Experimental results and analysis

4.1. Results

Various classification metrics such as Accuracy, Precision (Positive Predictive Value), F1-Score, Sensitivity (Recall), and Specificity are used to compare the performance of various models trained in the study. They paint a good picture of these model's efficiencies.

The metrics used in this work can be defined like this:

Table 1 illustrates that VGG-19, AlexNet, MobileNet-V2, and ResNet152V2 achieved decent accuracy scores of 92.25%, 95.05%, 97.59%, and 97.52%, respectively, while the proposed model achieved 98.38% accuracy. Since the proposed classifier is trained in two stages, the first phase, in which DenseNet-201 architecture is used to classify NON-COVID and COVID CT slices, the accuracy was 98.39%, and the second phase, in which InceptionV3 architecture is used to classify Normal and Pneumonia CT slices, achieved 99.98% accuracy. Other classification metrics are computed based on the potential outcomes of test data gathered by Confusion Matrix. It represents the number of counts from expected and actual values. The outcome of any classification problem may be either positive or negative. The confusion matrix has four primary outputs: True Positive (TP), True Negative (TN), False Positive (FP), and False Negative (FN). Cases in which the model predicted correct outcomes are denoted by TP, while cases in which the model predicted negative outcomes correctly are denoted by TN. FP denotes instances

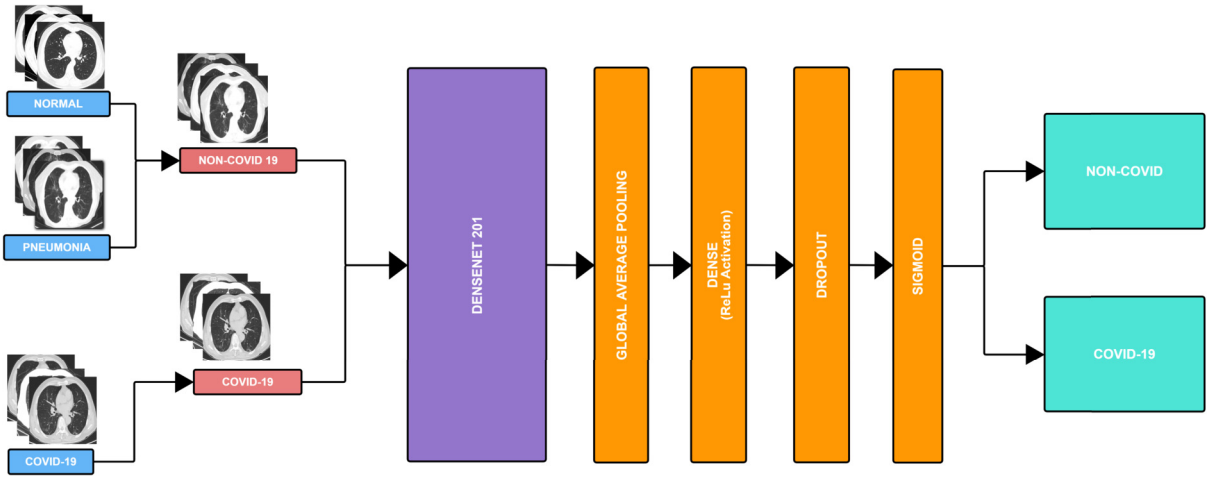

Fig. 5. Flowchart depicting the workflow of Phase-1.

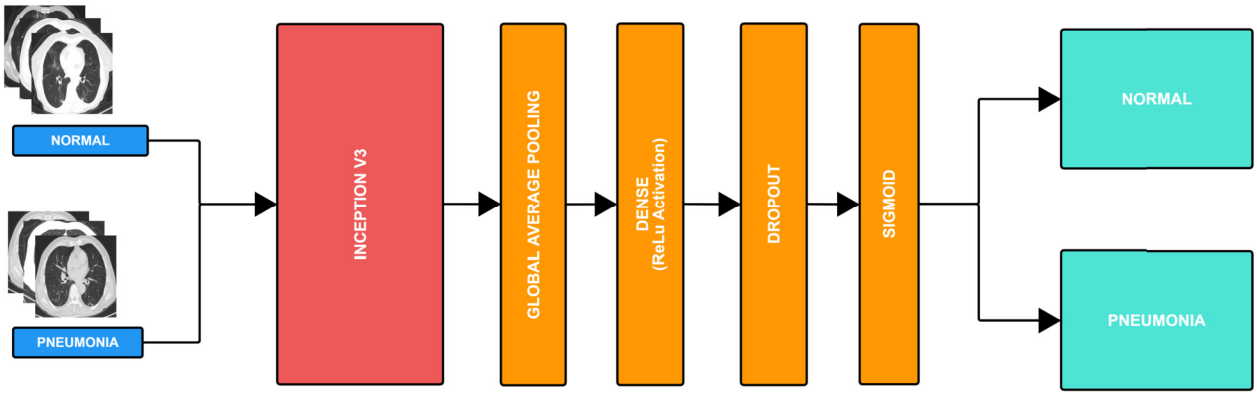

Fig. 6. Flowchart depicting the workflow of Phase-2.

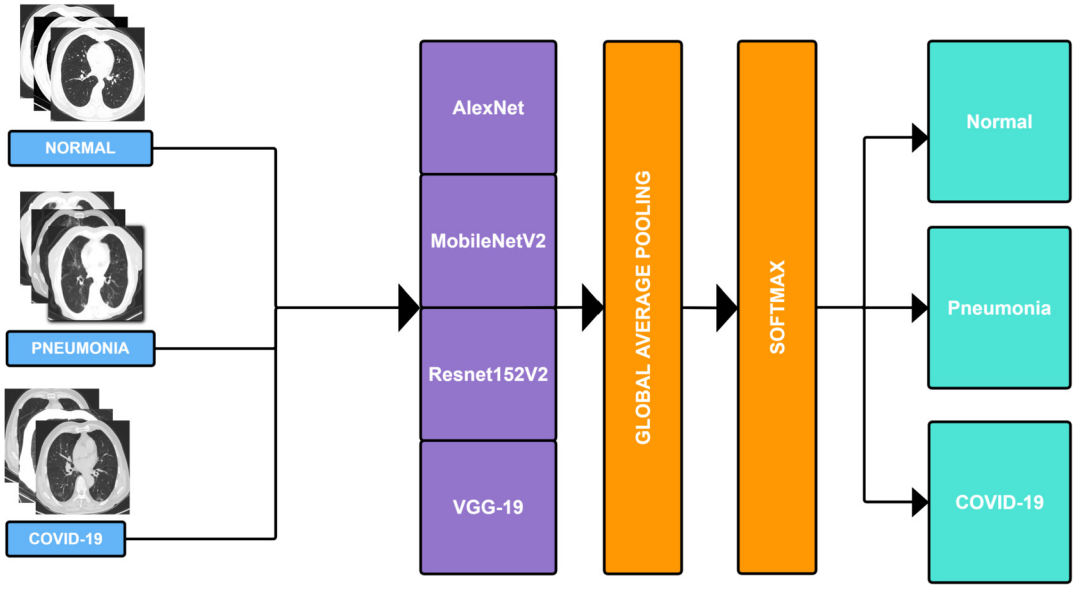

Fig. 7. Flowchart depecting workflow for Models.

Table 1
Accuracies of Various Models.

Model	No. of parameters	Accuracy (%)
VGG19	20,025,923	92.25
AlexNet	3,750,723	95.05
ResNet152 V2	58,194,051	97.52
MobileNetV2	2,227,715	97.59
Proposed Model	**40,246,690**	**98.38**

Table 2
PPV Values of Different Models.

Model	Positive Predictive Value (PPV) (%)		
	Normal	Pneumonia	COVID
VGG19	95.95	90.54	84.55
AlexNet	95.97	95.29	92.88
ResNet152 V2	98.10	98.79	94.62
MobileNetV2	98.00	96.43	98.20
Proposed Model	**98.99**	**99.56**	**95.62**

Table 3
Sensitivity Values of Different Models.

Model	Sensitivity (%)		
	Normal	Pneumonia	COVID-19
VGG19	93.94	91.89	86.70
AlexNet	97.92	95.96	88.50
ResNet152 V2	99.05	96.65	95.43
MobileNetV2	99.24	98.98	92.81
Proposed Model	**99.40**	**97.50**	**97.42**

where the model predicts positive but the outcomes are actually negative, while FN denotes instances where the model detects negative but the outcomes are actually positive.

Since the confusion matrix obtained from the two phases is 2×2, certain calculations were performed to adjust the results to a 3×3 confusion matrix from which all the parameters are evaluated. The false positives in the confusion matrix that were predicted as COVID-19 but had an actual label in the NON-COVID category were put in the final confusion matrix [Fig. 11] based on their actual label, which may be normal or pneumonia.

All of the true negatives and false negatives shown in the confusion matrix of Fig. 10 were fed into the phase-2 trained model, which was used to identify NON-COVID images as normal or pneumonia. The true negatives in the first row and first column of the confusion matrix had true labels of normal and pneumonia, while the false negatives present in the second row and first column had true labels of COVID-19 and were false predictions of the phase-1 model.

These incorrect predictions had to be passed on to the phase-2 model in order to determine whether the false prediction was pneumonia or normal in the NON-COVID group. Fig. 10 depicts the final result of these false predictions in the form of a 3×3 confusion matrix. Figs. 8 and 9 depicts the final output of the true negatives that were also transferred separately in a different 2×2 confusion matrix.

Positive Predictive Value (PPV) is the ratio of true positive predictions to the total actual positive values. Accuracy is defined as the proportion of accurate predictions made to actual predictions made. The major difference between Accuracy and PPV (Precision) is that precision reflects how measurable calculations are, while accuracy portrays how accurate a calculation is to a known or approved value. The Sensitivity or Recall of a prediction indicates how many of the actual predictions are correctly classified. It is also called True Positive Rate. High sensitivity implies few false negatives, resulting in missed patients with COVID-19 infections, while high PPV implies few false positives, adding an additional

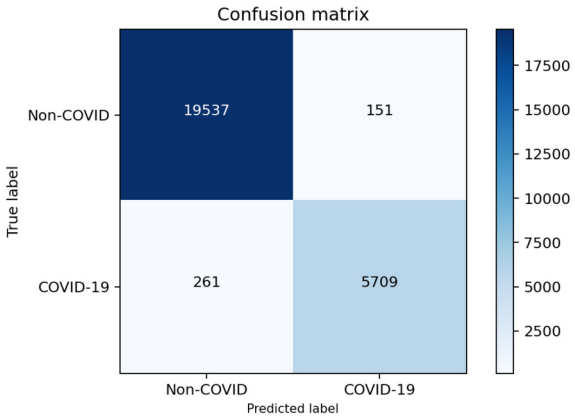

Fig. 8. Confusion Matrix – Phase-1.

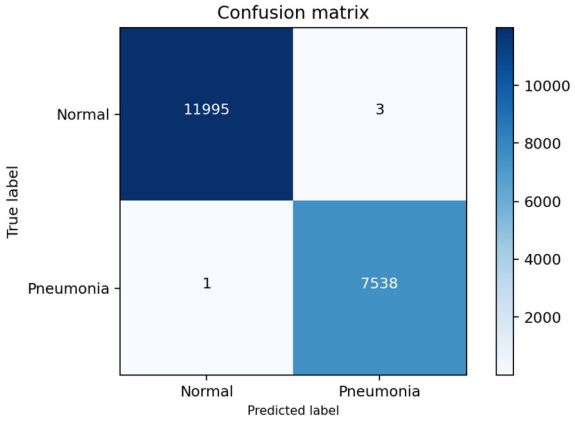

Fig. 9. Confusion Matrix – Phase-2.

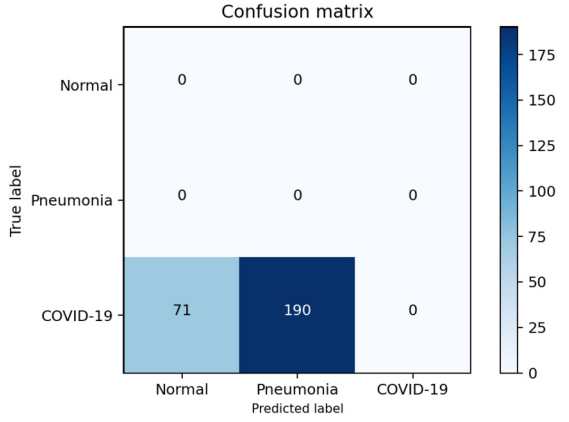

Fig. 10. False Negatives Confusion Matrix.

strain to the health care system, which has been strained due to the current pandemic. According to Tables 2 and 3, the proposed model has high COVID-19 sensitivity as compared to other models, (97.42%) and MobileNetV2 has a higher PPV value followed by the proposed model (98.20% and 95.62%).

$$Accuracy = \left(\frac{TP + TN}{TP + TN + FP + FN}\right)$$

$$PPV = \left(\frac{TP}{TP + FP}\right)$$

$$Sensitivity = \left(\frac{TP}{TP + FN}\right)$$

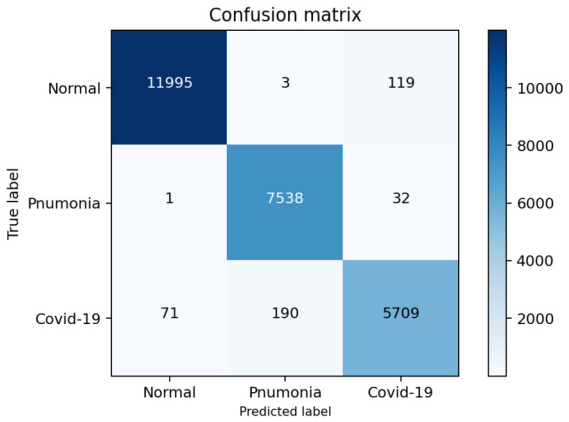

Fig. 11. Final Confusion Matrix.

Table 4
Specificity Values.

Model	Specificity (%)		
	Normal	Pneumonia	COVID-19
VGG19	96.31	96.06	95.35
AlexNet	96.45	98.03	97.80
ResNet150 V2	98.31	99.49	98.37
MobileNetV2	98.23	98.52	99.44
Proposed Model	**99.10**	**99.81**	**98.68**

Table 5
F1-Score Values.

Model	F1 – Score (%)		
	Normal	Pneumonia	COVID-19
VGG19	94.94	91.21	85.61
AlexNet	96.94	95.63	90.64
ResNet152 V2	98.57	97.71	95.02
MobileNetV2	98.62	97.69	95.43
Proposed Model	**99.19**	**98.52**	**96.57**

The ratio of true negatives to the total number of negatives is known as Specificity. It is also known as the True Negative Rate. It represents the cases in which the model expected a negative outcome when it was actually a negative outcome. The F1-Score is a blend of precision and sensitivity, with equal weightage for both metrics. It is the harmonic mean of precision and sensitivity (Recall). It is used to measure the model's relative efficiency. As compared to other models, the proposed model has a higher COVID-19 f1-score (96.57%). The MobileNetV2 model has considerably higher specificity than the proposed model. (99.44% and 98.68%) (From Tables 4 and 5).

$$Specificity = \left(\frac{TN}{TN + FP}\right)$$

$$F1\ score = 2 \times \left(\frac{PPV \times Sensitivity}{PPV + Sensitivity}\right)$$

It is clear that the proposed model outperforms many other CNN models, with an accuracy of 98.38% and sensitivity of 97.42% trained on the COVIDx-CT-2 dataset containing 1,94,922 images. These results can help to explain the potential utility of the proposed model for COVID detection automation.

Figs. 12–15 illustrate the Confusion Matrices of other models trained on the same data but using multi class classification.

Figs. 16 and 18 depict accuracy plots, while Figs. 17 and 19 depict loss plots of phase-1 and phase-2 respectively, all of which are plotted against the number of epochs.

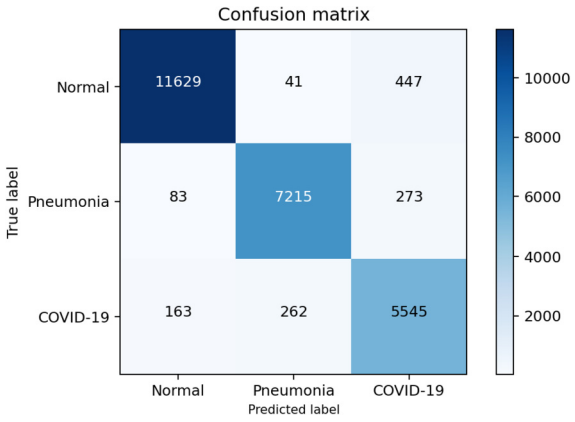

Fig. 12. Confusion Matrix – AlexNet.

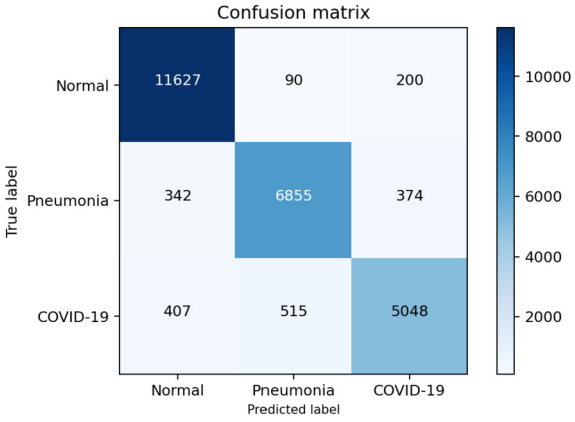

Fig. 13. Confusion Matrix – VGG-19.

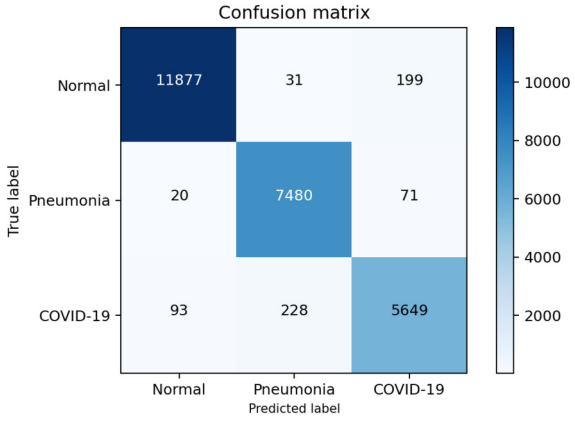

Fig. 14. Confusion Matrix – ResNet V2.

5. Conclusion

The significant proportion of proposed Deep Learning models for COVID detection were either binary classification or multiclass classification [4,10,27,34,19,37,7,13], [2], [33,24,30], but the proposed model was designed using two binary classifications. The use of two binary classifications rather than a single multiclass classification in our proposed model assisted us in minimizing false predictions of Pneumonia classes that were being classified to COVID images and vice versa. This reduction was achieved by classifying pneumonia and normal images as NON-COVID and then predicting an image as COVID positive or COVID negative in phase 1 and similarly predicting Pneumonia positive or Pneumonia negative in phase 2, resulting in improved accuracy. Improved accuracy

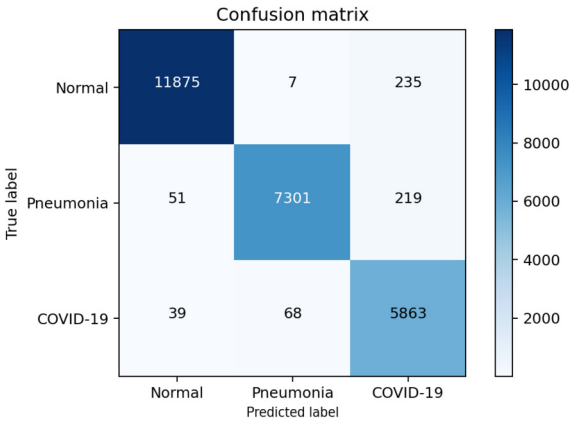

Fig. 15. Confusion Matrix – MobileNet V2.

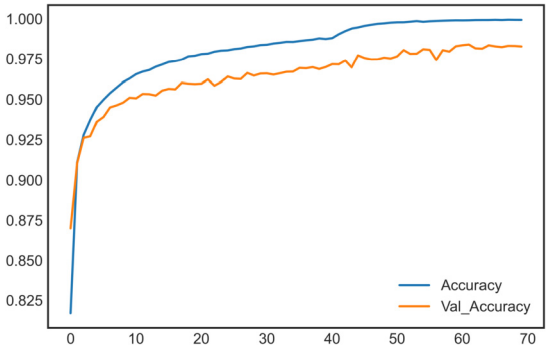

Fig. 16. Phase-1; Accuracy vs Epochs.

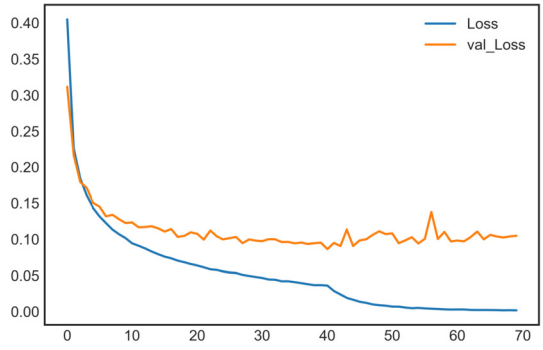

Fig. 17. Phase-1; Loss vs Epochs.

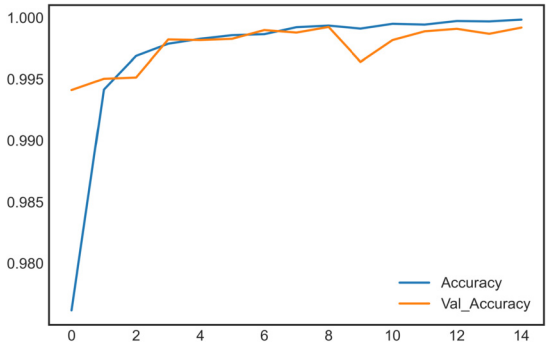

Fig. 18. Phase-2; Accuracy vs Epochs.

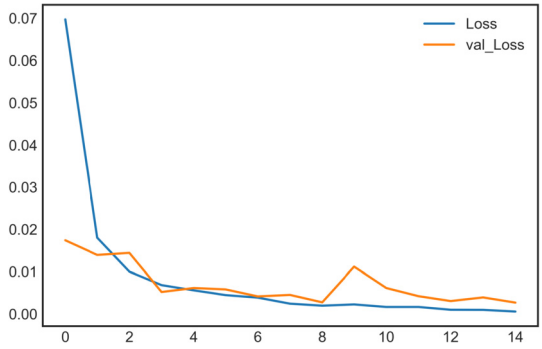

Fig. 19. Phase-2; Loss vs Epochs.

implies that the model is quite effective. It also has high sensitivity and F1-scores, which means less false negatives, which is crucial for infection control because a COVID positive patient who is falsely diagnosed COVID negative will spread the infection significantly. This model can be very beneficial at this time because prediction takes much less time than the RT-PCR test and is therefore, far more cost effective, assuming that accuracy and sensitivity are not compromised. However, this model can only be used for research purposes and is not yet ready for production. Although the model is far more accurate and performs exceptionally well, it should not be relied on blindly; patients should seek confirmation from a trained clinician or radiologist. This work could be improved, and many researchers could find it useful in their work.

Human and animal rights

The authors declare that the work described has not involved experimentation on humans or animals.

Informed consent and patient details

The authors declare that this report does not contain any personal information that could lead to the identification of the patient(s) and/or volunteers.

Funding

This work did not receive any grant from funding agencies in the public, commercial, or not-for-profit sectors.

CRediT authorship contribution statement

Sanskar Hasija: Conceptualization, Methodology, Software, Validation. **Peddaputha Akash:** Data curation, Formal analysis, Investigation, Writing – original draft. **Maganti Bhargav Hemanth:** Software, Writing – original draft. **Ankit Kumar:** Data curation, Writing – original draft. **Sanjeev Sharma:** Conceptualization, Methodology, Supervision, Writing – review & editing.

Declaration of competing interest

The authors declare that they have no known competing financial or personal relationships that could be viewed as influencing the work reported in this paper.

References

[1] M. Abadi, A. Agarwal, P. Barham, E. Brevdo, Z. Chen, C. Citro, G.S. Corrado, A. Davis, J. Dean, M. Devin, S. Ghemawat, I. Goodfellow, A. Harp, G. Irving, M. Isard, Y. Jia, R. Jozefowicz, L. Kaiser, M. Kudlur, J. Levenberg, D. Mane, R. Monga, S. Moore, D. Murray, C. Olah, M. Schuster, J. Shlens, B. Steiner, I. Sutskever, K. Talwar, P. Tucker, V. Vanhoucke, V. Vasudevan, F. Viegas, O. Vinyals, P. Warden,

M. Wattenberg, M. Wicke, Y. Yu, X. Zheng, Tensorflow: Large-scale machine learning on heterogeneous distributed systems, arXiv:1603.04467, 2016.
[2] A. Abbasian Ardakani, A. Kanafi, U.R. Acharya, N. Khadem, A. Mohammadi, Application of deep learning technique to manage Covid-19 in routine clinical practice using ct images: results of 10 convolutional neural networks, Comput. Biol. Med. 121 (2020), https://doi.org/10.1016/j.compbiomed.2020.103795.
[3] R.H. Abiyev, M.K.S. Ma'aitah, Deep convolutional neural networks for chest diseases detection, J. Healthc. Eng. 2018 (2018).
[4] T.B. Alakus, I. Turkoglu, Comparison of deep learning approaches to predict Covid-19 infection, Chaos Solitons Fractals 140 (2020) 110120, https://doi.org/10.1016/j.chaos.2020.110120.
[5] J.G.A. Barbedo, G.B. Castro, A study on CNN-based detection of psyllids in sticky traps using multiple image data sources, AI 1 (2020) 198–208.
[6] T.B. Chandra, K. Verma, B.K. Singh, D. Jain, S.S. Netam, Coronavirus disease (Covid-19) detection in chest x-ray images using majority voting-based classifier ensemble, Expert Syst. Appl. 165 (2021) 113909.
[7] M.E.H. Chowdhury, T. Rahman, A. Khandakar, R. Mazhar, M.A. Kadir, Z.B. Mahbub, K.R. Islam, M.S. Khan, A. Iqbal, N.A. Emadi, M.B.I. Reaz, M.T. Islam, Can AI help in screening viral and Covid-19 pneumonia?, IEEE Access 8 (2020) 132665–132676, https://doi.org/10.1109/ACCESS.2020.3010287.
[8] J. Deng, W. Dong, R. Socher, L. Li, K. Li, L. Fei-Fei, Imagenet: a large-scale hierarchical image database, in: 2009 IEEE Conference on Computer Vision and Pattern Recognition, 2009, pp. 248–255.
[9] Y. Fan, K. Zhao, Z.L. Shi, P. Zhou, Bat coronaviruses in China, Viruses 11 (2019) 210.
[10] H. Gunraj, A. Sabri, D. Koff, A. Wong, Covid-net CT-2: enhanced deep neural networks for detection of Covid-19 from chest CT images through bigger, more diverse learning, arXiv:2101.07433, 2021.
[11] H. Gunraj, L. Wang, A. Wong, Covidnet-ct: a tailored deep convolutional neural network design for detection of Covid-19 cases from chest CT images, Front. Med. 7 (2020) 1025, https://doi.org/10.3389/fmed.2020.608525, https://www.frontiersin.org/article/10.3389/fmed.2020.608525.
[12] K.F. Haque, A. Abdelgawad, A deep learning approach to detect Covid-19 patients from chest x-ray images, AI 1 (2020) 418–435.
[13] A.U. Ibrahim, M. Ozsoz, S. Serte, F. Al-Turjman, P.S. Yakoi, Pneumonia classification using deep learning from chest x-ray images during Covid-19, Cogn. Comput. (2021) 1–13.
[14] A.M. Ismael, A. Şengür, Deep learning approaches for Covid-19 detection based on chest x-ray images, Expert Syst. Appl. 164 (2021) 114054.
[15] M. Jamshidi, A. Lalbakhsh, J. Talla, Z. Peroutka, F. Hadjilooei, P. Lalbakhsh, M. Jamshidi, L.L. Spada, M. Mirmozafari, M. Dehghani, A. Sabet, S. Roshani, S. Roshani, N. Bayat-Makou, B. Mohamadzade, Z. Malek, A. Jamshidi, S. Kiani, H. Hashemi-Dezaki, W. Mohyuddin, Artificial intelligence and Covid-19: deep learning approaches for diagnosis and treatment, IEEE Access 8 (2020) 109581–109595, https://doi.org/10.1109/ACCESS.2020.3001973.
[16] A. Krizhevsky, I. Sutskever, G.E. Hinton, Imagenet classification with deep convolutional neural networks, Adv. Neural Inf. Process. Syst. 25 (2012) 1097–1105.
[17] P. Lakhani, B. Sundaram, Deep learning at chest radiography: automated classification of pulmonary tuberculosis by using convolutional neural networks, Radiology 284 (2017) 574–582, https://doi.org/10.1148/radiol.2017162326, pMID: 28436741.
[18] M. Lin, Q. Chen, S. Yan, Network in network, arXiv:1312.4400, 2014.
[19] X. Mei, H.C. Lee, K. Diao, M. Huang, B. Lin, C. Liu, Z. Xie, Y. Ma, P.M. Robson, M. Chung, A. Bernheim, V. Mani, C. Calcagno, K. Li, S. Li, H. Shan, J. Lv, T. Zhao, J. Xia, Q. Long, S. Steinberger, A. Jacobi, T. Deyer, M. Luksza, F. Liu, B.P. Little, Z.A. Fayad, Y. Yang, Artificial intelligence-enabled rapid diagnosis of Covid-19 patients, medRxiv: the preprint server for health sciences, https://doi.org/10.1101/2020.04.12.20062661, 2020.
[20] B. Nigam, A. Nigam, R. Jain, S. Dodia, N. Arora, B. Annappa, Covid-19: automatic detection from x-ray images by utilizing deep learning methods, Expert Syst. Appl. 176 (2021) 114883.
[21] Y. Pan, H. Guan, S. Zhou, Y. Wang, Q. Li, T. Zhu, Q. Hu, L. Xia, Initial CT findings and temporal changes in patients with the novel coronavirus pneumonia (2019-ncov): a study of 63 patients in Wuhan, China, Eur. Radiol. 30 (6) (2020) 3306–3309, https://doi.org/10.1007/s00330-020-06731-x. EpubFeb 13.
[22] H. Panwar, P. Gupta, M.K. Siddiqui, R. Morales-Menendez, V. Singh, Application of deep learning for fast detection of Covid-19 in x-rays using ncovnet, Chaos Solitons Fractals 138 (2020) 109944, https://doi.org/10.1016/j.chaos.2020.109944.
[23] R.R. Selvaraju, M. Cogswell, A. Das, R. Vedantam, D. Parikh, D. Batra, Grad-cam: visual explanations from deep networks via gradient-based localization, Int. J. Comput. Vis. 128 (2019) 336–359, https://doi.org/10.1007/s11263-019-01228-7.
[24] V. Shah, R. Keniya, A. Shridharani, M. Punjabi, J. Shah, N. Mehendale, Diagnosis of Covid-19 using CT scan images and deep learning techniques, medRxiv URL: https://www.medrxiv.org/content/early/2020/07/11/2020.07.11.20151332, 2020, https://doi.org/10.1101/2020.07.11.20151332, https://www.medrxiv.org/content/early/2020/07/11/2020.07.11.20151332.full.pdf.
[25] P. Simard, D. Steinkraus, J.C. Platt, Best practices for convolutional neural networks applied to visual document analysis, in: Seventh International Conference on Document Analysis and Recognition, 2003, Proceedings, 2003, pp. 958–963.
[26] K. Simonyan, A. Zisserman, Very deep convolutional networks for large scale image recognition, arXiv preprint arXiv:1409.1556, 2014.
[27] Y. Song, S. Zheng, L. Li, X. Zhang, X. Zhang, Z. Huang, J. Chen, H. Zhao, Y. Jie, R. Wang, et al., Deep Learning Enables Accurate Diagnosis of Novel Coronavirus (Covid-19) with CT Images, MedRxiv. 2020.
[28] K. Suzuki, Overview of deep learning in medical imaging, Radiol. Phys. Technol. 10 (2017) 257–273.
[29] M. Toğaçar, B. Ergen, Z. Cömert, Covid-19 detection using deep learning models to exploit social mimic optimization and structured chest x-ray images using fuzzy color and stacking approaches, Comput. Biol. Med. (2020) 103805, https://doi.org/10.1016/j.compbiomed.2020.103805.
[30] B. Wang, S. Jin, Q. Yan, H. Xu, C. Luo, L. Wei, W. Zhao, X. Hou, W. Ma, Z. Xu, Z. Zheng, W. Sun, L. Lan, W. Zhang, X. Mu, C. Shi, Z. Wang, J. Lee, Z. Jin, M. Lin, H. Jin, L. Zhang, J. Guo, B. Zhao, Z. Ren, S. Wang, W. Xu, X. Wang, J. Wang, Z. You, J. Dong, AI-assisted CT imaging analysis for Covid-19 screening: building and deploying a medical AI system, Appl. Soft Comput. 98 (2021) 106897, https://doi.org/10.1016/j.asoc.2020.106897.
[31] K. Weiss, T.M. Khoshgoftaar, D. Wang, A survey of transfer learning, J. Big Data 3 (2016) 1–40.
[32] Y. Xie, X. Wang, P. Yang, S. Zhang, Covid-19 complicated by acute pulmonary embolism, Radiol. Card. Imaging 2 (2020) e200067, https://doi.org/10.1148/ryct.2020200067.
[33] X. Xu, X. Jiang, C. Ma, P. Du, X. Li, S. Lv, L. Yu, Q. Ni, Y. Chen, J. Su, G. Lang, Y. Li, H. Zhao, J. Liu, K. Xu, L. Ruan, J. Sheng, Y. Qiu, W. Wu, T. Liang, L. Li, A deep learning system to screen novel coronavirus disease 2019 pneumonia, Engineering 6 (2020) 1122–1129, https://doi.org/10.1016/j.eng.2020.04.010.
[34] S.S. Yadav, S.M. Jadhav, Deep convolutional neural network based medical image classification for disease diagnosis, J. Big Data 6 (2019) 1–18.
[35] M.D. Zeiler, R. Fergus, Visualizing and understanding convolutional networks, in: European Conference on Computer Vision, Springer, 2014, pp. 818–833.
[36] R. Yamashita, M. Nishio, R.K.G. Do, et al., Convolutional neural networks: an overview and application in radiology, Insights Imaging 9 (2018) 611–629, https://doi.org/10.1007/s13244-018-0639-9.
[37] K. Zhang, X. Liu, J. Shen, Z. Li, Y. Sang, X. Wu, Y. Zha, W. Liang, C. Wang, K. Wang, et al., Clinically applicable AI system for accurate diagnosis, quantitative measurements, and prognosis of Covid-19 pneumonia using computed tomography, Cell 181 (2020) 1423–1433.